J. Expt. & Clin. Anat. 5(2): 47-60 (2006).

JECA

Effects Of BCG Vaccination On The Morphometry Of Pancreatic Islets Of Langerhans Of Streptozotocin-Treated Diabetic Rats

[1]*STEPHEN O. ADEWOLE, [2]EZEKIEL A. CAXTON-MARTINS, [3]ABDUKADIR A. SALAKO AND [4]OLADEPO W. DOHERTY

*[1]Departments of Anatomy and [2]Cell Biology, Faculty of Basic Medical Sciences, College of Health Sciences, Obafemi Awolowo University, Ile-Ife, Osun State, Nigeria

[3]Department of Surgery, Faculty of Clinical Sciences, College of Health Sciences and

[4]Department of Chemistry, Faculty of Sciences, Obafemi Awolowo University, Ile-Ife, Osun.

*Author for correspondence

ABSTRACT

Immune-mediated (type 1) diabetes mellitus (IMD) is an autoimmune disease resulting from chronic destruction of pancreatic â-cells by autoreactive T lymphocytes. Although there has been much advancement in diabetes management, targeting the precise etiology of the disease process has remained elusive. Recent progress in the understanding of the immunopathogenesis of IMD, however, has led to new intervention strategies, especially antigen-based therapies given as altered peptide ligands (APL) or as vaccines. There have been many attempts at immunologic modulation as a block or prevention of the underlying process. Recent evidence from animal studies has raised the possibility that immunization by vaccines can influece the pathogenesis of type 1 diabetes mellitus. In non-obese diabetic (NOD) mice and biobreeding (BB) rats, complete Freund's adjuvant (CFA) and Bacille Calmette-Guérin (BCG) vaccines have successfully been used to interrupt or prevent the onset and recurrence of type 1diabetes. In this study, we investigated the effect of BCG vaccination on multiple low dose streptozotocin-induced diabetes (MLDS) in mice, with particular emphasis on the immunohitochemistry and morphometry. The mice were pretreated with BCD vaccine, 7 days before starting multiple low dose stretpozotocin (STZ). We observed the effects of BCG vaccination on the body weight, blood glucose concentration, serum insulin, pancreatic insulin contents and quantitative analysis of islet morphology/viability of the STZ-induced insulitis after the animals were sacrificed. The findings of the present study showed that BCG-treated mice improved in body weights, serum insulin, pancreatic insulin contents and reduced blood glucose concentration. There was also a reduction in the level of â-cell apoptosis, and a significant ($p < 0.05$) increase in â-cell regeneration, and â-cell mass. Our results suggest that BCG vaccination exerts some positive effects in the diabetic state by proving cellular integrity of islet cells, and drastically reducing the development of insulitis and overt diabetes in MLDS diabetic mice.

Keywords: Immunoregulation; MLDS; Mycobacterium; Morphology; Apoptosis; Regeneration; BCG vaccination; Type 1 Diabetes.

Immune-mediated (type 1) diabetes mellitus (IMD) is a polygenic, environmentally influence autoimmune disease that results from the chronic destruction of insulin-secreting pancreatic â-cells by autocreative T lymphocytes (Bach, 1994; Mathis et al., 2001). Strong environmental influences are coupled with multiple weak susceptible genes, resulting in numerous defects in immuno-regualtion that jeopardize tolerance self. The life-time risk of type 1 diabetes approaches one in 250 (Melton et al; 1983), and despite advances in disease management, the many complications that result from long-standing IMD imposes increased morbidity and mortality rates. The incidence rates vary widely, probably due to ethnic, genetic, geographic and environmental differences. Type 1 diabetes mellitus (T1DM) is the third most prevalent severe chronic disease of childhood, after asthma and mental retardation, affecting 0.% of the general population by the age of 20 and 0.5-1% during the life-span (Rewers et al., 1988). The incidence increases by 3-5% per year, approximately 1.4 million in the U.S., and 10 20 million people globally suffer from T1DM (DERIG, 1990).

The process of destruction of pancreatic â-cells is chronic in nature, often starting in infancy and continuing over many months to years prior to onset of disease. It is estimated that some 80% of â-cells have been ablated by the time of clinical diagnosis, while the islets that

remain at that time have a chronic inflammatory infiltration referred to as insulitis. This insulitis consists mostly of $CD8^+$ T cells in addition to variable numbers of CD4+ T cells, B lymphocytes, macrophages,and natural killer (NK) cells (Atkinson and Maclaren, 1994). In non-obese diabetes (NOD) mice, the insulitis lesion starts outside of the islets and then moves internally, with macrophages being the earliest invaders. The islet cells over-express class 1 major histocompatibility complex (MHC) and become hypervascular as the process continues. The distribution of islets with insulitis within the pancreas of newly diagnosed IMD and NOD mice is not uniform (Foulis et al., 1986).

Autoantibodies to â-cells and their antigens are collectively seen as islet cell cytoplasmic antibodies (ICA). Autoantibodies to insulin (IAA), like ICA, can be detected in peripheral blood years before diabetes develops, by immunofluorescence microscopy (Riley et al., 1990). Major constituents of ICA are antibodies against the enzyme glutamic acid decarboxylase (GAD), the insulinoma-associated antigen-2 (IA-2) and a homologous and antigen, IA-2â. GAD promotes glutamate conversion to the neurotransmitter gamma amino butyric acid (GABA), while IA-2 and IA-2â are structurally related transmembrane proteins of the tyrosine phosphatase family of enzymes, which are 70% homoglous in their antigenic intracellular region (Kukreja and Maclaren, 1999).

Antigen presenting cells (APC) such as dendritic cells, B lymphocytes and macrophages have been shown to play roles in the progression of insulitis and IMD. Dendritic cells present peptide antigens to naïve T cells, and are important in shaping immune response. They are among the first cells to appear in both rodent and human insulitis. B lymphocytes also play an important role in generating MHC class II-restricted T cell responses to certain antigens. They secrete autoantibodies that bind to pancreatic antigens and trigger NK cell-mediated cytolysis. Macrophages secrete interleukin (IL)-2, thereby stimulating $CD4^+$ T cells to secrete interferon (IFN-ã and IL-2. IFN-ã stimulates other resting macrophages to release other cytokines such as IL-1â, tumor necrosis factor (TNF)-á, and free radicals, which are destructive to pancreatic insulin-secreting â-cells. Helper T-cell clones (Th1, Th2), also activate CD4+ T-cell and Th1 produces interleukin (IL)-2, interferon (IFN)-ã and lymphotoxin, whereas Th2 cell expresses IL-4, IL-5, IL-6 and IL-10, albeit in individual human 'Th' cells there is much overlap (Romagnani, 1992).

There have been many studies investigating the use of various forms of mycobacterium to confer protection against diabetes (Sadelain et al., 1990; Harada et al., 1990). Infection of NOD mice with viable Mycobacterium avium, prior to onset of diabetes, has been shown to protect them from developing diabetes (Martins and Aguas, 1996). Infection with M. avium was found to enhance IL-4 secreting T cells, suggesting potential efficacy of mycobacterium-based therapies. Other investigators have explored the role of cross-reactivity with a mycobacterial 65-kDa heat shock protein in the pathogenesis of diabetes. Vaccination with this molecule could down-regulate immunity and prevent development of diabetes (Elias et al., 1991). Immunization with M. bovis-BCG has been reported not only to protect NOD mice from diabetes (harada et al., 1990), but has also been shown to prevent insulitis in streptozotocin (STZ)-induced diabetic mice (Baik et al., 1999). In contrast, however, human studies with BCG given to patients with newly diagnosed IMD have not been successful in preserving â-cell function (Allen et al., 1999; Elliott et al., 1998). Sadelain et al., (!990) reported that a single injection of complete Freund's adjuvant (CFA; water-in-oil emulsion containing heat-killed M. tuberculosis) given at 5 weeks to NOD mice, prevented diabetes without any additional therapy. In that study, CFA was found to induce regulatory cell in the spleen that produced a transient global reduction of lymphocyte proliferative responses. Despite preservation of insulin-producing â-cells, however, there was still infiltration of the islet cells with

mononuclear cells, albeit with enhanced Th2 phenotype.

An intensive trial of pork insulin therapy given to NOD mice from 4 weeks of age until 180 days of age powerfully prevented them from developing diabetes (Atkinson and Maclaren, 1990). Pancreatic histology showed considerable peri-islet inflammation but little intra-islet penetration or â-cell loss. One possible explanation for the prevention of destruction was that â-cell 'rest' brought about by suppression of autoantigen expression on the islet cells, thereby minimizing their ability to be recognized immunologically and destroyed. With the beneficial effects received with insulin alone or adjuvant alone, other trials sought to vaccinate with antigen plus adjuvant, and showed protective effect on NOD mice (Muir et al., 1995). Oral and intranasal antigens such as whole insulin, â-chain insulin, or GAD can suppress development of diabetes in NOD mice (Maron et al., 1999; Polanski et al., 1997).

Within the endocrine pancreas, once the insult of autoimmunity is abrogated, the physiologic process of regeneration can continue efficiently, eventually replenishing the population of insulin-producing cells to a number sufficient to maintain euglacemia. In view of this point, this study aimed at investigating the protective effects of BCG vaccination on the endocrine pancreatic islet cells by comparing alterations in blood glucose levels, â-cells mass, insulin content as well as morphometric configuration in the endocrine pancreas, following BCG vaccination of multiple low dose stretozotocin-treated diabetic mice.

MATERIALS AND METHODS

Animals

Fifty healthy adult mice, 10 15 weeks old and weighing 35 40g, were used. The animals were kept and maintained under standard laboratory conditions of temperature, light and humidity; and were allowed free access to food (standard pellet diet) and water ad libitum. The animals were randomly assigned to three experimental groups: A (control), B (diabetic), and C (diabetic + BCG). All the animals were fasted for 16 hours, but still allowed free access to water, before the commencement of our experiments. The control group of animals (A) consisted of ten mice, while the treatment groups consisted of forty mice.

Maintenance and treatment of animals were in accordance with the principles of the "Guide for care and use of laboratory animals in research and teaching" prepared by the National Institute of Health (NIH) publication 86-23 revised in 1985.

Induction Of Diabetes And BCG Vaccination

Group C animals were intradarmally inoculated with BCG (0.5ml) vaccine (Aventis Pasteur, Toronto, Canada) 7 days before the induction of diabetes (Yagi et al., 1991). Diabetes mellitus was induced (in groups B and C diabetic 'test' mice) by multiple intraperitoneal injections of STZ (35mg/kg, freshly dissolved in 0.1mol/1 citrate buffer, pH 6.3), for consecutive five days (Rossini et al; 1977). Control mice were injected with only citrate buffer solution intraperitoneally. The 'test' animals in both groups B and C became diabetic within 8 days after STZ administration. Diabetic state was confirmed by measuring basal blood glucose concentration 5 days after the last STZ injection. At the end of the 16 hour fasting period taken as zero time (i.e., 0 hour), blood glucose levels (initial glycaemia G_0) of the fasted normal (normoglycemic) and STZ-treated, diabetic (hyperglycemic) mice were determined and recorded.

Glucose And Insulin Estimations

Blood samples were obtained by repeated needle puncture of the same tail tip vein. Samples were obtained 1 day before STZ-treatment, and on various days after induction of diabetes mellitus. Diabetes was allowed to develop and stabilize in these STZ-treated mice over a period 5 10 days. Blood glucose concentrations were determined by means of Bayer Elite® Glucometer, and compatible blood glucose test strips (Henry, 1984). The mean fasting blood glucose levels for normal,

nondiabetic mice were found to vary between 4.01 ± 0.04 and 4.20 ± 13mmol/L. Fasted STZ-treated mice with blood glucose concentrations > 18mmol/L were considered to be diabetic, and used in this study. The blood glucose concentration of STZ + BCG-treated mice was 6.8 + 0.4mmol/L. The serum insulin concentration were measured radioimmunoassay (RIA) kit (Diagnostic Products Corporation, Los Angeles, CA, USA), using purified rat insulin as standard (Novo, Copenhagen, Denmark).

Histological Procedures

Pancreatic tissues were harvested from the sacrificed animals fixed in aqueous Bouin's solution, and were sequentially embedded in paraffin blocks according to the standard procedure, sectioned at 5μm thickness, and then stained for functional pancreatic â-cells with Aldehyde Fuchsin Trichrome (Mowry et al; 1980).

Immunohistochemistry And Morphometry

The animals were sacrificed by cervical dislocation, some at the end of the 16 hours fasting period, and others on various days following STZ administration. Pancreatic tissues were excised and weighed after the fat and lymphnodes had been removed. The splenic parts of the pancreas of each mouse were fixed in aqueous Bouin's solution and embedded in paraffin. Each pancreatic block was serially sectioned (5μm) throughout its length to avoid any bias due to changes in islet distribution or cell composition, and thereafter mounted on slides. For each pancreas, 10 sections were randomly chosen at a fixed interval through the block (every 30th section), a procedure that has been shown to ensure that selected sections are representative of the whole pancreas (Mossavat et al; 1997). Sections were immunostained for insulin, using a peroxidase indirect labeling technique. The sections were incubated for 1hr with guinea-pig anti-insulin serum (final dilution 1:1,000, Ref. 64-104-1; Aurora, OH). Thereaftrer, sections were incubated for 45min with peroxidase-conjugated rabbit anti-guinea pig IgG (final dilution 1:20; Dako, Carpinteria, CA). The activity of the antibody-peroxidase complex was revealed with 3,3'-diaminobenzidine-tetrahydrochloride, using a peroxidase substrate kit (DAB; Biosys-Vector, Compiegne, France). A standard concentration of hematoxylin was added as a counterstain.

Quantitatively, measurement of cell parameters was made by means of image-analytical software (Analysis 3.0; Soft Imaging System, Mûster, Germany). Four serial sections were obtained from each level for each of the pancreatic hormone. All the sections were introduced in the Compaq PC computer, using an analog Sony Video camera (PAL system), after being converted to the red-green-blue (RGB) system necessary for digitalizing and processing the sections. The totality of islets found was considered for each section, an image being generated for each islet detected. For this purpose, a X25 objective was used. The islets under approximately 40 μm in diameter were not measured since they were considered possible error factors, as it could not be determined whether they were islets superficially cut or small groups of 4 to 5 cells. These measurements were recorded and processed automatically, and the following parameters were afterwards calculated: volume density (VD=Ó cell area/RA) and cell density (CD = number of cells/RA). Both of them were referred to different reference areas (RA): endocrine reference area (RA_e) and total pancreas area (RAt). RAe represents the total endocrine area scanned, in which islet populations were scored. Then, with the (Ó) of the areas (A) of each endocrine â-cell, referred to as RAe, we obtained the respective VD, which indicated cell mass, according to a usually accepted concept. We also calculated the VD of the endocrine pancreas and the VD of â-cell, taking the total pancreas as a reference area (RAt), which was outlined including the intraglandular adipose tissue, and excluding the connectinve interlobular septa, the larger vessels and nerves, as well as extraglandular adiposity. The use of this new image analysis system has increased the accuracy of measurements and reduced the overestimation of â-cell size found

with the planimetry program (Montanal et al; 1993, Nacher et al; 1998).

Pancreatic Insulin Content Determination

The splenic regions of the pancreatic tissues from euthanized mice were weighed and homogenized, on various experimental days, in acid-ethanol solution (75% ethanol, 23.5% distilled water, 1.5% concentrated HC1). After overnight incubation at 4°C the suspensions were centrifuged, and the supernatants were collected and assayed for insulin content, using a competitive ELISA kit (Kekow et al; 1988). Plates were coated with rabbit anti-guinea-pig Ig secondary Ab (Organon Teknoka, Durban, NC), followed by incubation with a guinea-pig anti-human insulin Ab (Cortex Biochem, San Leandro, CA). Following two washing steps, various extract dilutions or insulin standards (Linco Research, St. Louis, MO) were mixed with constant concentration of HRP-conjugated rat insulin (Organon Teknika) for 4h at room temperature, or at 40C overnight, before competitive capturing was allowed for 3hrs. after washing five times, Sigma FAST OPD tablets (Sigma, St. Louis, MO) were used as substrate. Results were analyzed using ceres 900 ELISA-readers.

Beta-Cell Area

Beta-cell area was measured in the same sections used for â-cell mass, replication, or apoptosis quantification. The perimeter of the â-cell tissue on a random field was carefully traced on the computer's monitor to exclude any other tissue, and the total â-cell area in that field was measured. Then, the â-cell nuclei in the same field were counted (202 $\pm$ 12 nuclei per sample). To calculate the area of individual â-cell, the total â-cell area in the field was divided by the number of â-cell nuclei.

Beta-Cell Mass

Beta-cell mass was measured by point-counting morphometry (Weibel, 1979) on the same immunoperoxidase-stained sections used to determine â-cell apoptosis, using a 48-point grid to obtain the number of intercepts over â-cell, over endocrine non-â-cells and over other tissues. Beta-cell mass was obtained by multiplying the total pancreatic weight by the relative â-cell volume.

Beta-Cell Apoptosis

Apoptotic cells were detected using the terminal deoxyribonucleotidyl transferase-mediated dUTP nick-end labeling (TUNEL) technique with the Apop tag in situ cell death detection kit (Appligene-Oncor, Illkirch, France). Sections were pretreated with proteinase K (20ìg/ml) for 20min at room temperature and washed with double-distilled water. Thereafter, the sections were incubated with terminal deoxyribonucleotidyl transferase (TdT) enzyme and digoxigenin-nucleotide residues for 1h at 37°C. After washing the slides in phosphate-buffered saline (PBS), pH 7.4, they were incubated with a peroxidase-conjugated anti-digoxigenin antibody and stained with 3,3'-diaminobenzidine-tetrahydrochloride using a peroxidase substrate kit DAB. Sections were then incubated for 1hr with a mixture of three different antibodies: rabbit and anti-swine glucagons (final dilution 1:1,000), rabbit anti-human somatostain (final dilution 1:1,600,ICN, Biochemicals), and rabbit anti-human pancreatic polypeptide (final dilution 1:1,500, ICN, Biochemicals). Sections were then incubated for 45mins with alkaline phosphatase conjugated goat anti-rabbit IgG (final dilution 1:150, Biehringer, Carpinteria, CA). The activity of antibody-alkaline phosphatase complex was revealed with an alkaline phosphatase substrate kit. Sections were counterstained with hematoxylin and mounted in Eukitt. Apoptosis causes cell shrinkage and fragmentation, leading to loss of cell integrity. Therefore, apoptotic â-cells may be degranulated in the last phases of apoptosis. Furthermore, apoptosis is a rapid process, with less than 1hr of morphological evidence (Coles et al; 1993). Thus measurement of apoptotic â-cell rate with a direct insulin staining could lead to an underestimation of this rate. We used the staining of non- â-cells to surround the core of the islet and identify the â-cells. On stained

sections, the islet tissue was identified as a mantle of endocrine non-â-cells with red cytosol, and apoptotic positive cells with brown nuclei. No nuclei staining were found in controls in which TdT enzyme was omitted. Most of the endocrine apoptotic cells were located in the core of the islets, delimited by non-â-cell immunostaining, suggesting that they were apoptotic â-cells.

For each pancreas, multiple parallel sections were analyzed in five levels, each 0.5mm apart, to minimize sample error. On average, 100 islets were analyzed per pancreas. Insulitis was graded by a quadripartite scale: 0; no insulitis; 1, peri-insulitis; 2, moderate insulitis with disrupted islet architecture containing insulin-producing â-cells; and 3, complete destructive insulitis with few or no insulin positive cells. An insulitic score was computed for each pancreas by summing the insulitis grade for each islet and dividing the sum by the total number of islets examined.

Beta-Cell Replication

Pancreatic sections that had not been used for morphometric studies were used to measure â-cell replication rates. 5-bromo-2'deoxyuridine (BrdU; Sigma) is incorporated in newly synthesized DNA and therefore labels replicating cells. A 6h BrdU incorporation interval was chosen to avoid the possibility of including daughter cells (Swenne, 1982). Sections were double-stained for $BrdU^+$ using a cell proliferation kit (Amersham International, Amersham, UK) and for insulin. Sections were, thereafter incubated with a mouse monoclonal antibody anti-BrdU diluted in a nuclease solution (according to the kit protocol) for 1h at room temperature, and washed with Tris 0.05M, pH 7.6. Thereafter, the sections were incubated with an affinity-purified peroxidase anti-mouse IgG and stained with 3,3'-diaminobenzidine-tetra-hydrochloride' using a per oxidase substrate kit DAB.

Sections were subsequently incubated with guinea-pig anti-insulin antibody for 1h as described above and then with alkaline phosphatase-conjugated goat anti-guinea pig IgG for 45 mins (final dilution 1:150, Sera Lab, Carpinteria, CA). The activity of the antibody alkaline phosphatase complex was revealed with an alkaline phosphatase substrate kit (Biosys-Vector). Sections were counterstained with hematoxylin and mounted in Eukitt.

On these sections, â-cells showed red cytosol and $BrdU^+$ cells appeared with brown nuclei. A minimum of 1100 â-cell nuclei were counted per section at a final magnification of X1000. The proportion of BirdU+ â-cell nuclei to the total â-cell nuclei was calculated. The result represents the percentage â-cell replicative rate in a 6h interval.

Statistical Analysis

Data obtained from 'test' mice treated with STZ alone, STZ + BCG-treated as well as those obtained from citrate buffer-treated 'control' mice, were pooled and expressed as means ($\pm$ SEM). Differences between the means were analyzed statistically with one-way analysis of variance (ANOVA; 95% confidence interval). Value of $p < 0.05$ were taken to imply statistical significance.

RESULTS

Characteristic of diabetic state

Five days after the last STZ administration, all the animals that were treated with STZ displayed glucosuria, hyperglycemia, hypoinsulinemia and moderate loss of body weight. The pancreatic weight, plasma glucose, plasma insulin, and pancreatic insulin contents of control, STZ-treated diabetic and STZ + BCG-treated mice were either significantly increased or decreased ($p < 0.05$) in value, respectively (Table1).

Blood Glucose And Serum Insulin Concentration

In our control set of experiments, pretreatment of the mice with citrate buffer alone did not significantly modify ($p > 0.05$) the serum insulin and blood glucose concentrations. As shown in Fig. 1 and Table 3, there was a gradual rise in the blood glucose concentrations of the STZ-treated mice as from day 5 following

injection of STZ, and the values were significantly higher ($P<0.05$) than those of control animals. Furthermore, higher levels of blood glucose concentrations of the STZ-treated mice were persistently observed throughout the study period (18.2 ± 0.1 mmol/L). The blood glucose concentrations in the BCG vaccine pre-treated group C, (6.8mmol/L) ·significantly reduced in value ($p<0.05$) when compared with STZ group B mice, and the reduction was observed throughout the study period. Serum insulin concentrations in the STZ-treated mice were significantly decreased (5.8± 1.12ìU/ml) when compared with normal group. The BCG vaccine treated group showed increase in suboptimal values of serum insulin (10.20 ± 1.20ìU/ml) and stabilized till the end of study period (Fig. 2, Table 3).

Histological Findings

Histologically, pancreatic islets of STZ-treated mice showed extensive changes, including distorted islets, â-cell death and atrophy, throughout the study period (Fig. 3B).

The islets also developed a remarkably accelerated insulitis (Fig. 5A), with diffused T cell infiltration by H & E staining; in keeping with MLDS, leading to autoimmune destruction of the islets, but exocrine pancreatic acinar epithelium, ductal and connective tissues appeared normal. Intriguingly, no lymphocyte infiltration was detected in islets of BCG-treated mice at any of the time examined (Fig. 5B). the severity of lymphocyte infiltration in the islets of STZ-treated mice was scored by the following grade: grade 0, normal; grade 1, periductal lymphocyte infiltrate; grade II, peri-insulitis; grade III, insulitis (lymphocytic infiltrate invading islets); grade IV, severe insulitis (massive lymphocytic infiltrate with islet destruction) (Baik et al; 1999). Most of the islets showing infiltration here were high grade, between grades III and IV (Fig. 5A).

Hormone Content In The Islets

Immunohistochemistry staining of the pancreatic tissues before STZ injection showed the presence of a strong islet insulin immunoreactivity at a level of 0.59 islet/mm^2 of total pancreatic tissue. This was limited to cytoplasmic staining of individual â-cells (Fig. 4A). The majority of islets from BCG-treated pancreases stained positive for insulin, suggesting that the architecture of BCG-treated mice was normal (Fig. 4C). in contrast, islet cells from diabetic mice were architecturally distorted, containing significantly fewer insulin-positive cells (Fig. 4B). Quantitative image analysis was used to assess the proportion of insulin positive cells per islet in STZ-treated pancreatic sections. The percentage of STZ-treated and BCG-treated islets stained for insulin were 46.26 ± 3.2% and 78.56 ± 24% ($p<0.05$) respectively (Fig. 4B and C). Together, these findings further support that BCG vaccination protected islets from destruction.

Of the most interesting is the stability of pancreatic insulin content of the BCG-treated mice (13.2± 2.0ìU/mg), in contrast to the STZ-treated mice, insulin levels were ~55-fold higher. (Table 3,). This stability in pancreatic insulin values was also observed to reflect in the immunohistochemistry staining (Fig. 4C). Immunohistochemistry staining intensity was an evidence of replicative processes leading to increase in â-cell mass, regaining its normal immunostaining for insulin and functional status up to the day of normoglycemia.

Table 1. Various parameters recorded in STZ-diabetic, STZ + BCG-treated and control mice just before and after removal of pancreas. Values presented represent the means (+ SEM) of 10 observations.

Treatment groups	Body weight (g)	Pancreas weight (g)	Plasma glucose (mmol/L)	Serum insulin concentration (µU/ml)	Pancreatic insulin contents (µU/mg)
STZ-diabetic	36.3± 0.3*	0.19± 0.08*	18.20±0.1*	5.80±1.10*	7.2±1.4*
Control (ND)	40.6±0.5	0.28±0.06	4.20±0.6	12.4±2.10	15.3±2.6
STZ+BCG mice	39.8±0.4	0.22±0.04	6.80±0.4	10.20±1.20	13.9±2.0

Table 2: Total pancreatic α- and β-cell mass and β-cell area in STZ-treated mice and mice treated with BCG vaccine.

Groups	% β-cells	B-cell mass (mg/pancreas)	B-cell area (μm^2/ β-cell)	α-cell mass (mg/pancreas)
Control	0.5± 0.02	5.5± 0.6	391± 20	1.5±0.2
STZ-treated	0.2±0.04[a]	2.0±0.02[a]	295±26[a]	1.3±0.3
STZ + BCG-treated				
Day 20	0.3±0.03	3.7±0.2	34±35	1.2±0.2
Day 40	0.5±0.02[b]	5.2±0.4[b]	386±09[b]	1.3±0.1
Day 60	0.4±0.01[b]	4.9±0.5[b]	379±34[b]	1.1±0.4

[a]$p < 0.05$, compared with diabetic control mice
[b]$p < 0.05$, compared with STZ – treated mice. Values are means (± SEM) of 8 mice.

Table 3: Changes in blood glucose concentrations and serum/pancreatic insulin contents in diabetic mice treated with BCG vaccine

Blood glucose concentration (mmol/L)							
	Control ←			**Treated** →			
Days	0	10	20	30	40	50	60
STZ-treated	4.2±06	16.8±0.2[a]	18.1±0.4[a]	17.8±0.3[a]	18.5±0.1[a]	18.7±0.3[a]	18.6±1.5[a]
STZ + BCG-treated	4.1±0.5	6.5±0.4[a]	7.2±0.1[a]	7.8±0.2[a]	7.6±0.3[a]	6.9±0.1[a]	6.8±0.3[b]
Serum insulin concentration (μU/ml)							
STZ-treated	12.2±1.2	8.5±2.2	6.3±1.4[a]	5.9±1.3[a]	5.7±2.3[a]	5.5±1.2[a]	5.6±1.5[a]
STZ + BCG-treated	12.4±2.3	9.9±1.1	9.8±2.1[a]	10.1±0.8[a]	10.2±0.9[a]	9.9±2.2[a]	11.3±1.5[b]
Pancreatic insulin content (μU/mg)							
STZ-treated	15.5±2.4	9.6±2.1	7.9±2.3[a]	7.6±1.3[a]	6.9±2.2[a]	6.7±1.4[a]	6.2±3.1[a]
STZ +BCG-treated	15.2±3.1	10.2±2.4	10.9±3.5[a]	11.8±2.1[a]	12.3±1.7[a]	12.9±3.1[a]	13.2±2.1[b]

[a]$p < 0.05$, compared with diabetic control mice
[b]$p < 0.05$, compared with STZ – treated mice. Values are means (± SEM) of 8 mice.

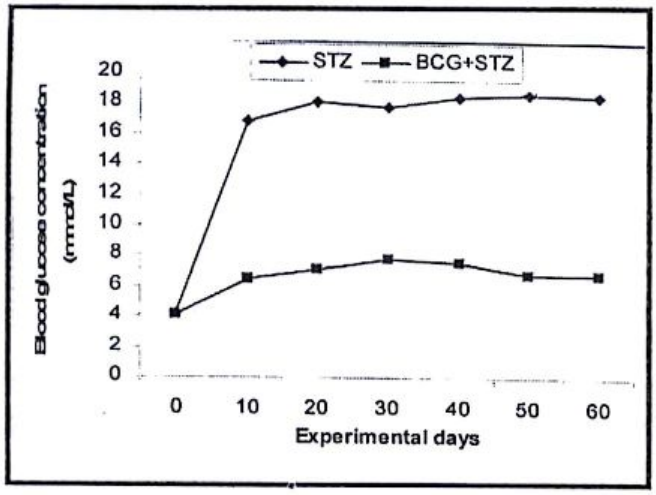

Figure 1. Blood glucose concentration in STZ-treated and BCG + STZ-treated mice. The figure illustrates persistent hyperglycemic state of STZ-diabetic mice; STZ + BCG-treated mice maintained normoglycemic condition throughout the study period.

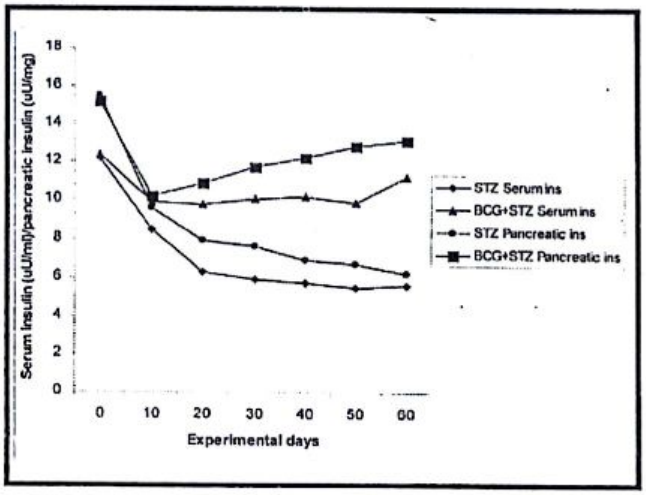

Figure 2. Serum insulin and pancreatic insulin in STZ-treated and BCG + STZ-treated mice. The figure illustrates protective effects of BCG on the insulin content of the pancreas and maintenances of normal serum insulin level.

Beta-cell mass and individual â-cell area

In STZ-treated mice, â-cell mass was decreased compared with control. The â-cell mass decreased was ~3-fold to control mice and ~2.5-fold to STZ-BCG treated mice to (Table 2). The â-cell mass increased gradually on days 20, 40 and 60 in BCG-treated mice to 3.7± 0.2, 5.2±0.4, 4.9±0.5mg respectively. No significant difference was observed in the á cell mass and in the distribution of glucagons cells in control group animals was 391 ± 20ìm^2. âeta-cell area significantly reduced ($p<0.05$) in STZ-treated mice (295 ± 26ìm^2), but significantly increased in BCG-treated mice 345±35, 386±0.9 and 379 ±34ìm^2 on days 20, 40 and 60 respectively.

Beta-cell apoptosis

Pancreata were analyzed by immunohistochemistry for evidence of apoptosis. Apoptotic B-cells were detectable with the DNA breakage labeling method (TUNEL technique) within the islet boundaries of STZ-treated mice. Intra-islet B-cell death was significantly ($p<0.05$) greater in STZ-treated mice (Fig. 6A). Apoptosis was limited to islets with insulitis in which there was approximately two to three apoptotic cells per islet section compared with infrequent apoptotic B-cells seen in STZ + BCG-treated islets (STZ + BCG-treated, 0.3±0.1/islet and STZ-treated 0.9±0.1/islet). Apoptotic B-cells in the BCG-treated group showed low level apoptosis, with remarkable B-cells cellularity (Fig. 6B).

Beta-cell replication

Beta-cell replication was normal in BCG-treated islets (0.32 ± 0.14%) compared with B-cell replication in control islets (0.36±0.08%). The STZ-treated islets showed insignificant ($p>0.05$) proliferative rate (0.24±0.12%) when compared with other two groups.

Figure 3. Aldehyde fuchsin trichrome staining of the pancreatic tissues. Arrows show B-cells with purple colour, while arrowheads show a-cells in orange colour. (A) Control group: showing normal cells in the islet of Langerhans and showing distinct granules filing the entire islet of Langerhans that are strongly stained purple, a-cells are seen mostly at the periphery (B) Diabetic untreated group: shrunken islet of Langerhans displaying degenerative and necrotic changes, nuclear shrinkage and pyknosis were evident with cytoplasmic vesiculation in the center of the islet of Langerhans, decreased cellular density. (C)STZ + BCG-treated: still retained

Figure 4. Immunohistochemistry staining of the pancreatic tissues, represented by dark granules. (A) Control group: showing B-cells in the islets of Langerhans that are strong staining with the anti-insulin antibody. Immunoperoxidase, haematoxylin counterstain. (B) Diabetic untreated group: showing shrunken islet with weak immunooreactive B-cells in the islet of Langerhans. Immunoperoxidase, haematoxylin counterstain. (C) STZ-BCG treated: still retained substantial amount of B-cells with remarkable anti-insulin antibody staining granules. Immunoperoxidase haematoxylin counterstain. Final magnification X 60.

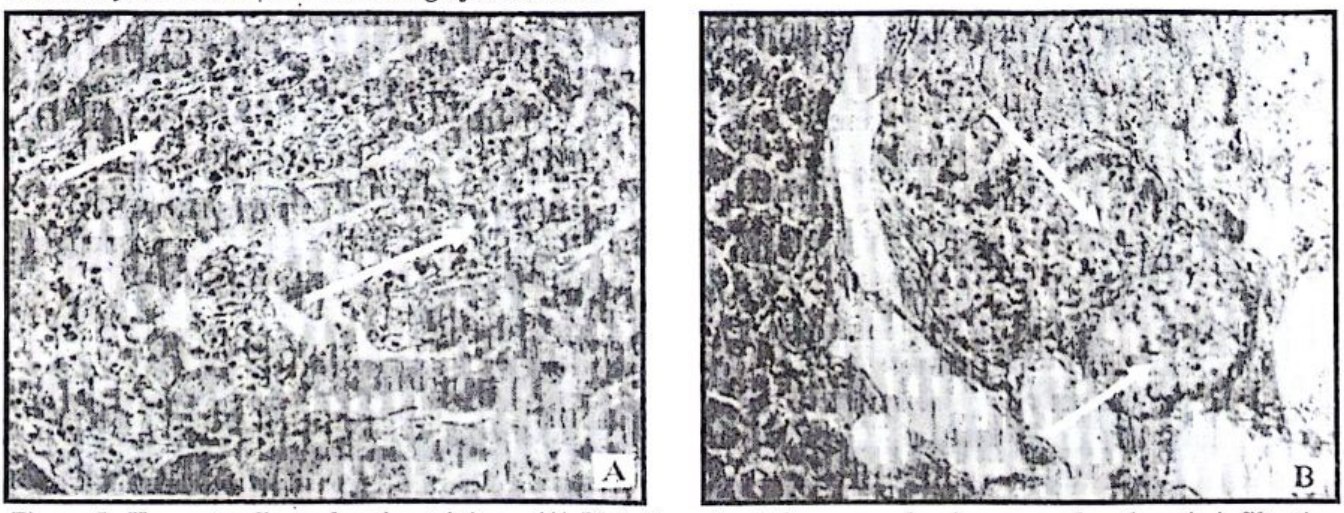

Figure 5: Haematoxylin and eosin staining. (A) Diabetic untreated group: showing severe lymphocytic infiltration (arrows) post MLDS, the entire islet of Langerhans is distorted with grade III IV insulitis (arrows showing lymphocytes). (B) STZ-BCG treated group: showing distinct islet of Langerhans with viable B-cells (arrows). Final magnification X 60.

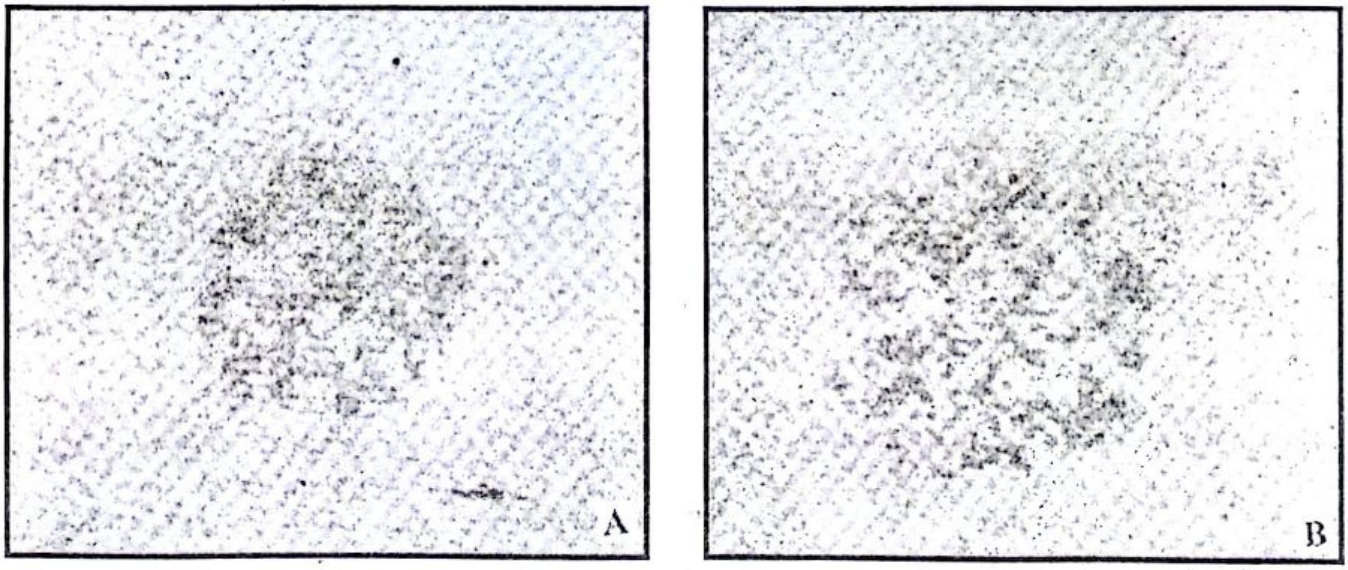

Figure 6: TUNEL-peroxidase-staining. (A) STZ-treated group: showing very scanty B-cells within the islet of Langerhans (X 120 magnification). (B) TUNEL^{+} nuclei stained with DAB of B-cells at the interface of lymphocyte infiltration (X 160 magnification)

DISCUSSION

Administration multiple low doses of treptozotocin has been successfully used to induce B-cell toxin to IDDM susceptible mice (Kim and Steinberg, 1984). One of the initial steps in the pathogenesis of autoimmune insulin-dependent diabetes mellitus is the adhesion of circulating cells of the immune system to islet endothelium (Hanninen et al; 1993, Itoh et al; 1993, Yang et al; 1996). Recruitment of these cells leads to insulitis with progressive B-cell destruction (Foulis et al; 1986, Roep et al; 1995).

A number of immunologic and environmental manipulations have been reported in a variety of animal models of autoimmune disease, including type 1 diabetes (muir and Ramiya, 1996; Semone et al; 1999). At first glance, the apparent effectiveness of this relatively large number of different strategies seems surprising (Sadelain et al; 1990). Intervention strategies that have been proposed include immune suppression, T cell modification, cytokine therapies, subcutaneous injections of insuline, B-chain peptide 9-23 of insulin, glutaic acid decarboxylase (GAD_{65}), islet cell cytoplasmic antibodies (ICA_{69}), dietary interventions, and antigen-based therapies or vaccines (Daniel and Wegmann, 1996; Ramiya et al; 1997). The broadening interest in vaccines to treat or prevent IMD has been particularly embraced and has led to the ongoing National Diabetes Prevention Trial-1 (DPT-1) (DPT-1 Study Group, 1995). In order to target the underlying causes of autoimmunity in IMD, there must first be good understanding of normal immune tolerance mechanisms since autoimmunity is actually a form of immune deficiency.

A new approach to prolonging insulin production in a newly diagnosed diabetic is through immunostimulation (Qin and Singh, 1997). This strategy is based on the lower incidence of diabetes in NOD mice stimulated immunologically with agents as diverse as allogeneic cells or the mycobacterial vaccine, *Bacilli Calmette-Guerin* (BCG) (Harada et al; 1990). The mechanism for the protection is not clear, although stimulation and expansion of populations of T cells producing IL4 or IL10 has been suggested (Harada et al; 1990). In the absence of clear evidence linking BCG antigens with those expressed by islet cells, the mechanism of action may well be immunologically nonspecific. It is possible that immune stimulation after the onset of diabetes might reduce insulin requirements or increase C-peptide synthesis when measure one year after vaccination with the attenuated mycobacterium, BCG. Vaccination with BCG is thought to be safe and is immunogenic, and a preliminary small human study gave some evidence for benefit in preserving C-peptide (Allen et al; 1998). A report by Benifacio et al; 2005) indicates that neonatal BCG vaccination did not influence the development of islet autoantibodies in a prospectively followed cohort of offspring of patients with type 1 diabetes (Huppmann et al; 2005). Treatments to islet cell destruction and prevent diabetes would ideally be started before the beta-cell mass is significantly compromised. Nevertheless, detecting partial benefit in recent-onset diabetics would be useful if it is a precursor to an intervention that could be used with greater efficiency in subjects with pre-type 1 diabetes. Ultimately, the focus of the prevention of diabetes must be in patients with pre-type 1 diabetes (Warram et al; 1984).

The results of antigenic immunostimulatory studies in NOD mice hold great promise for similar beneficial effects in humans who have just begun to develop the clinical disease or are at risk for IMD (Tisch et al; 1998). Current investigations will determine if antigen based therapies can in fact abrogate ongoing autoimmunity via immunostimulation and ultimately prevent diabetes in humans without the risk of general immunosuppression. If successful, the dream of the diabetes vaccine will indeed be a future that was realized (Elliot et al; 1994).

Much evidence shows that B-cell apoptosis is a fundamental process involved in the pathogenesis of type 1 diabetes (Augstein et al; 1998, Mandrup-poulsen, 2001). The accelerated course disease allowed us to

determine by direct in situ histological staining of unmanipulated pancreatic tissue that pancreatic B-cells die by apoptosis as a result of lymphocytic infiltration. In this study, we provide evidence that BCG vaccination responded in converting a destructive B-cells into a non-destructive form of auto-immunity. Functionally, BCG does not prevent or reverse autoimmunity directed against islet tissue, although they do prevent development of insulin-dependent diabetes (Shehadeh et al; 1993). We have also shown that mice vaccinated with BCG did not develop overt diabetes, characterized by normoglycemia, intact B-cells displaying high insuline content, and absence of B-cell specific T-cell activation. The finding of essentially total protection from pancreatic B-cell damaga in BCG vaccinated mice is remarkable. An exaggerated B-cell damage was observed in STZ-treated mice, therefore, the apoptotic cells may be a critical determinant contributing to the initiation of autoimmunity by having the capacity to instruct APCs to modulate immune responses so that the outcome is T-cell activation (Albert, 2004, Savill et al; 2002). Theoretically, any destruction causing antigen to be shed and presented by nearby APCs may provide an opportunity for B-cell-specific T cells to become activated in predisposed individuals. For example, coxsakie virus infection has been associated with autoimmune diabetes in both human and animal models (June and Yoon, 2001). In keeping with our results, it has been shown that virus-mediated bystander tissue damage can induce immune activation against B-cells much like STZ-induced autoimmune destruction of the islets (Horwitz et al; ;2002, Anreoletti et al; 1997).

Apoptosis was specific to B-cell in infiltrated islets only (see Table 2). Apoptosis is limited to the B-cells at or near the interface between the lymphocytic infiltrate and intact islet tissue, indicating that either direct cell-cell contact or localized production of cytokines could mediate B-cell killing. However, our data has shown that BCG vaccination avert apoptosis and remarkably improve cellular integrity and functional status of the islet cells.

The mechanisms underlying prevention of spontaneous diabetes, induced diabetes and recurrence of diabetes by mycobacterial preparation (BCG or CFA) is complex. It may involve induction of regulatory cells, cytokine switch and T cell apoptosis (Qin et al; 1998, Ryu et al; 2001). On the other hand, down-regulation of diabetogenic T cells by BCG may also involve induction of T cell anergy, peripheral delection and/or induction of regulatory cells.

In conclusion, our study provides clear evidence that, BCG immunotherapy in STZ-diabtic mice averts overt diabetes, drastically reduced B-cell apoptosis, insulitis and improved cellular integrity of islet cells. Our findings also indicate that B-cell mass is an important component of islet function in normal mice. In diabetic mice, the failure of maturating factors during rapid pancreatiac regeneration may prevent improvement of insulin secretion.

Acknowledgements

The authors are grateful to Messrs Adeogun Oludele, Ibe Joseph and Izobo Stanley for their technical assistance in tissue processing.

REFERENCES

Albert ML (2004). Death-defying immunity: do apoptotic cells influence antigen processing and presentation. Nat Rev Immunol. 4:223-231.

Allen H, Klingensmith G, Jensen P, Simoes E, Hayward A, Chase H (1998). Effect of Bacelle Calmette-Guerin vaccination on new-onset type 1 diabetes. A randomized clinical study. Diabtes Care 22:1703-1707.

Andreoletti L, Hober-Vandenberghe C, Belaich S, Vantyghem MC, Lefebvre J, Wattre P (1997). Detection of coxsackie B virus RNA sequences in whole blood samples from adult patients at the onset of type 1 diabetes mellitus. J. Med. Virol. 52:121-127.

Augstein P, Elefanty AG, Allison J, Harrison LC (1998). Apoptosis and B-cell destruction in pancreatic islets of NOD mice with spontaneous and cyclophosphamide-accelerated diabetes. Diabetlogia 41;1381-1388.

Atkinson M and Maclaren N (1994). The pathogenesis of insulin-dependent diabetes mellitus. N Engl J Med. 331:1428-1436.

Bach JF (1994). Insulin-dependent diabetes mellitus as an autoimmune disease. Endocr Rev. 15:516-542.

Baik S, Park I, Choi K, Kim Y, Kim N, Kim S, Song G and Choi D (1999). BCG vaccine prevents insulitis in low dose streptozotocin-induced diabetic mice. Diabetes Res Clin Pract 46:91-97.

Coles H, Burne J and Raff M (1993). Large-scale normal cell death in the developing rat and its reduction by epidermal growth factor. Developmental 118:777-784.

Daniel D and Wegmann DR (1996). Protection of nonobese diabetic mice from diabetes by intranasal or subcutaneous administration of insulin peptide B-(9-23). Proc. Natl Acad Sci. USA. 93:956-960.

Diabetes Epidemiology Research International Group (DERIG) (1990). Secular trends in incidence of childhood IDDM in 10 countries. Diabetes. 39:858-64.

DPT-1 Study Group (1995). The Diabetes Prevention Trial-Type 1 diabetes (DPT-1): implementation of screening and staging of relatives. Transplant Proc. 27:33-77.

Elias D, Reshef T, Birk O, Van dZR Walker M and Cohen I (1991). Vaccination against autoimmune mouse diabetes with a T-cell epitope of the human 65-kDa heat shock protein. Proc Natl Acad Sci USA 88:3088-3091.Elliott J, Marlin K and Couch R (1998). Effect of Bacille Calmette-Guerine vaccination on C-peptide secretion in Children newly diagnosed with IDDM. Diabetes Care 21:1691-1693.

Elliot J, Qin H, Bhatti S et al. (1994). Immunization with the larger form of mouse glutamic acid decarboxylase (GAD 67) prevents autoimmune diabetes in NOD mice. Diabetes. 43: 1494-1499.

Foulis A, Liddle C, Farquharson M, Richmond J and Weir RS (1986). The histopathology of the pancreas in type 1 (insulin-dependent) diabetes mellitus: a 25-year review of death in patients under 20 years of age in the United Kingdom. Diabetologia. 29:267-274.

Hanneinen A, Salmi M, Simell O and Jalkanen S (1993). Edothelial cell-binding properties of lymphocytes infiltrated into human diabetic pancreas. Implications for pathogenesis of IDDM. Diabetes 42:1656 1662.

Harada M, Kishimoto Y and Makino S (1990). Prevention of overt diabetes and insulinitis in NOD mice by a single BCG vaccination. Diabetes. 8:85-90.

Henry JD (1984). "Clinical diagnosis and management by laboratory methods". 17th Ed., P. 1433.

Horwitz MS, Ilic A, Fine C, Rodriguez E and Sarvetnick N (2002). Presented antigen from damaged pancreatic beta cells activates autoreative T cells in virus-mediated autoimmune diabetes. J. Clin. Investig. 109:79-87.

Huppmann M, Baumgarten A, Ziegler AG and Boniface E (2005). Neonatal Bacille Calmette-Guerin vaccination and type 1 diabetes. Diab Care 28(5): 1206.

Itoh N, Hanafusa T, Miyazaki A, Miyagawa JI, Yamagata K, Yamamoto K, Waguri M, Imagawa A, Tamura S, Inada M, Kawata S, Tarui S, Kono N and Matsuzawa Y (1993). Mononuclear cell infiltration and its relation to the expression of major histocompatibility complex antigens and adhesion molecules in pancreas biopsy specimens from newly diagnosed insulin-dependent diabetes mellitus patients. J. Clin. Invest. 92:2313-2322.

Jun HS, Yoon JW (2001). The role of virus in type 1 diabetes: two distinct cellular and molecular pathogenic mechanisms of virus-induced in animals. Diabetologia 44:271-285.

Kekow J, Urichs K, Muller-Ruchholtz W, Gross WL (1988). Measurement of rat's insulin: enzyme-linked immunosorbent assay with increased sensitivity, high accuracy, and greater practicability than established radioimmunoassay. Diabetes, 37:321P.

Kim YT, Steinberg C (1984). Immunologic studies on the induction of diabetes in experimental animals: cellular basis for the induction of diabetes by streptozotocin. Diabetes 33:771.

Kukreja A, Maclaren N (1999). Autoimmunity and diabetes. J. Clin Endocrinol Metab 84:4371-4378.

Mandrup-Poulsen T (2001). B-cell apoptosis: stimuli and signaling. Diabetes. 50:S58-S63.

Maron R, Melican N, Weiner H (1999). Regulatory TH2-type T cell lines against insulin and GAD peptides derived from orally and nasally-treated NOD mice suppress disabetes. J. Autoimmune 12:251-258.

Martins T, Aguas A (1996). Changes in B and T lyphocytes associated with mycobacterium-induced protection of NOD mice from diabetes. J. Autoimmuni 9:501-507.

Mathis D, Vence L and Benoist C (2001). B-cell death during progression to diabetes. Nature 414:792-798.

Melton LD, Palumbo P, Chu C (1983). Incidence of diabetes mellitus by clinical type. Diabetes Care. 6:75-86.

Montana E, Bonner-Weir S, Weir GC (1993). B-cell mass and growth after syngeneic islet cell transplantation in normal and streptozotocin diabetic C57BL/6 mice. J Clin Invest 91:780-787.

Movassat D, Saulnier C, Portha B (1997). Insulin administration enhances growth of the B-cell mass in streptozotocin-treated newborn rat. Diabetes 46:1445-1452.

Mowry RW, Longley JB and Emmel VM (1980). Only aldehyde fuchsin made from pararosanilin stains pancreatic granules and elastic fibers in unoxidized microsections: problems caused by unlabelling of certain basic fucsins. Stain Technol., 55:91-103.

Muir A, Peck A, Clare-Salzler M, Song Y, Cornelius J, Luchetta R, Krischer J, Maclaren N (1995). Insulin immunization of NOD mice induces protective insulitis characterized by diminished intra-islet interferon-gamma transcription. J. Clin. Invest. 95:628-634.

Muir A, Raniya V (1996). New strategies in oral immunotherapy for diabetes prevention. Diabetes Metab Rev. 12:12-1.

Nacher V, Merino JF, Raurell Soler E, Monanya E (1998). Normoglycemia restores B-cell replicative response to glucose in transplanted islets exposed to chronic hyperglycemia. Diabetes 47:192-196.

Polanski M, Melican N, Zhang J and Weiner H (1997). Oral administration of the immunodominant B-chain of insulin reduces diabetes in the NOD mouse and is associated with a switch from Th1 to Th2 cytokines. J Autoimmun 10:339-346.

Qin H-Y, Singh B (1997). BCG vaccination prevents insulin-dependent diabetes mellitus (IDDM) in NOD mice after disease acceleration with cyclophosphamide. J Autoimmunity 10:271-278.

Qin H-Y, Elliott JF, Lakey JR and Singh B (1998). Endogenous immune response to glutamic acid decarboxylase (GAD67) in NOD mice is modulated by adjuvant immunotherapy. J. Autoimmunity 11:591.

Ramiya VK, Lan MS, Wasserfall CH, Notkins AL and Maclaren NK (1997). Immunization therapies in the prevention of diabetes. J Autoimmun. 10:287-292.

Rewers M, LaPort RE, King H and Tuomilehto J (1988). Trends in the prevalence and incidence of diabetes: insulin-dependent diabetes mellitus in childhood. World Health Stat Q. 41:179-89.

Riley W, Maclaren N, Krischer J, Spillar R, Silverstein J, Schatz D, Schwartz S, Malone J, Shah S, Vadheim C et al. (1990). A prospective study of the development of diabetes in relatives of patients with insulin-dependent diabetes. N Engl J Med. 323:1167-1172.

Roep BO, Kallan AA, Duinkerken G, Arden SD, Hutton JC, Bruining GJ, DeVries RRP (1995). T-cell reactivity to beta-cell membrane antigens associated with beta-cell destruction in IDDM. Diabetes 44:278-283.

Romagnani S (1992). Human TH1 and TH2 subsets: regulation of differentiation and role in protection and immunopathology. Int. Arch Allergy Immunol 98:279-285.

Rossini AA, Like AA, Chick WL, Appel MC, Cahill GF (1977). Study of streptozotocin-induced insulitis and diabetes. Proc Natl. Acad. Sci. USA 74:2485.

Ryu S, Kodama S, Ryu K, Faustman DL (2001). Reversal of established autoimmune diabetes by restoration of endogenous beta cell function. J. Clin. Invest. 108:63.

Sadelain MW, Qin H-Y, Lauzon J, Singh B (1990). Prevention of type 1 diabetes in NOD mice by adjuvant immunotherapy. Diabetes. 39:583-589.

Savill J, Dransfield I, Gregory C, Haslett C (2002). A blast from the past: clearance of apoptotic cells regulates immune responses. Nat. Rev. Immunol. 2: 965-975.

Shehadeh N, Calcinaro F, Bradley BJ, Bruchilm J, Vardi P, Lafferty KJ (1993). Effect of adjuvant therapy on development of diabetes in mouse and man. Lancet 43: 706.

Simone EA, Wegmann DR, Eisenbarth GS (1999). Immunologic "vaccination" for the prevention of diabetes (type 1). Diabetes Care. 22(Suppl 2): B7-B15.

Swenne I (1995). The role of glucose in the *in vitro* regulation of cell cycle kinetics and proliferation of fetal pancreatic B-cells. Diabetes 31:754-760.

Tisch R, Liblau RS, Yang XD, Liblau P, McDevitt HO (1998). Induction of GAD65-specific regulatory T-cells inhibits ongoing autoimmune diabetes in nonobese diabetic mice. Diabetes. 47:894-899.

Warram JH, Krolewski AS, Gottlieb MS, Kahn CR (1984). Differences in risk of insuline-dependent diabetes in offspring of diabetic mothers and diabetic fathers. N Engl J Med 311(3):149-152.

Weibel RE (1979). Point counting methods. In *Serological Methods*. Vol. 1. London, Academic Press, p. 101-161.

Yagi H, Matsumoto M, Suzuki S, Misaki R, Suzuki R, Makino S, Harada M (1991). Possible mechanism of preventive effect of BCG against diabetes mellitus in NOD mouse: 1. Generation of suppressor macrophages in spleen cells of BCG-vaccinated mice. Cell Immunol. 138:130.

Yang XD, Michie SA, Mebius RE, Tisch R, Weissman IL, McDevitt HO (1996). The role of cell adhesion molecules in the development of IDDM. Implications for pathogenesis and therapy. Diabetes 45:705-710.

J. Expt. & Clin. Anat. 5(2): 61-63 (2006).

JECA

Scapula Morphometry Of Adult Nigerians In The Southeast

*[1]O.A. EGWU, [1]E O EWUNONU, [2]CIP ANIBEZE, [2]K N OVUOBA, [3]A C UGWU, [3]A.N. ETEUDO AND [1]AKPA A O C
[1]Department Of Anatomy, Ebonyi State University, Abakaliki, Nigeria Email: egwuoc@yahoo.com
[2]Department Of Anatomy, Abia State University, Uturu, Nigeria
[3]Department Of Radiology, Federal Medical Center, Abakaliki, Nigeria
*Author for correspondence

ABSTRACT

Twenty-five adult bony Scapulae of Nigerians were used to report detailed bony dimensions of the scapula. The average length of the scapulae was 146.24 ± 6.78mm. the mean spine length was 126.83 ± 7.29mm and acromial dimensions were 45.46 ± 4.03 x 21.91 ± 2.07 and 7.36 ± 1.30 thick (mm). Glenoid dimensions showed that anteroposterior diameter = 26.54 ± 1.86mm, superoinferior diameter = 37.72 ± 1. 65mm and diameter at glenoid constriction = 19.58 ± 1.35(mm). Coracoid dimensions were 39.20 ± 2.67mm x 9.30 ± 2.12 x 14.48 ± 1.36mm. The average diameter of scapular notch was 14.90 ± 2.94mm. also 52% of Scapula notch were U-shaped and 92% of acromion were curved. The average thickness of the lateral boarder was 11.72 ± 1.23mm. glenoid dimensions correlated with all acromial dimensions except the acromial thickness. This detailed study of scapula dimensions will provide information for surgical procedures and detection of significantly displaced scapular fracture.

Keywords: Scapula, Morphometry, Nigerians.

Physical anthropometrical measurements of bone and other organs have become relatively important in medicine (Didia et al, 2002). These measurements when obtained can be used to ascertain age, sex, and race. They equally serve as a guide in the detection of anomalies.

The scapula is a triangular bone that overlaps the second to seventh ribs on the posterolateral part of the thorax. Structurally, it connects the clavicle to the humerus forming part of the pectoral girdle. Embrologically, it derives from the somatic mesenchyme except its coracoid process, which is derived from the somatopleuric mesenchyme (Gumpel-Pinot, 1984).

The role of the scapula in maintaining upper extremity function cannot be overemphasized and so is the need for knowledge of its morphometric and Geometric anatomy. the morphometric anatomy of the scapula has been implicated in some shoulder joint anomalies, pathomechanics of some rotator cuff diseases (Mallon et al, 1992; Gumina et al, 1999). It equally has a lot of clinical relevance in total shoulder athroplasty and recurrent shoulder dislocation (Mallon et al, 1992). To the knowledge of the authors and search from Google internet search engine, there are no documented values for scapula dimensions of Nigerian adults. Hence, this study is designated to establish normal values of the dimensions scapula of Nigerian adults with a view to establishing a guide for plastic, orthopedic and reconstructive practices in shoulder replacement surgery as well as definition of osseous glenohumeral instability.

MATERIALS AND METHODS

Twenty-five (25) intact scapulae were collected from the Anatomy laboratory of Faculty of Basic Medical Sciences, Ebonyi State University, Abakaliki. The 25 bones were those of Nigerians who lived and were from Southeastern Nigeria.

On collection, the bones were washed and brushed in water using a detergent and then soaked in water at about 70°C for 6 hours. The bones were washed again with water and detergent to remove any left over tissue. Later, the bones were sun dried for four (4) days and then soaked in a mixture of 5 litres of water, 1 litre of bleach and 10% hydrogen peroxide (H_2O_2). Finally, the bones were sun dried for 8 days and measurements were carried out.

Measurements

The measurements were done using a pair of dividers and metric rule calibrated in millimeters. The measurements for each parameter was done by one scientist for three (3) times and the mean value obtained. This was to remove interobserver error and error due to parallax. The measured parameters include:

Scapula length (from superior angle to inferior angle). Distance from the base of the suprascapula notch to superior rim of glenoid cavity; thickness of the medial boarder at 1cm from the edge; length of the spine (from medial edge to lateral margin of the acromion); the anteroposterior width of the spine at 1cm and 4cm from the medial edge; acromial dimensions; coracoid dimensions and glenoid dimensions. Other parameters were diameter of scapula notch, and thickness of the lateral boarder. The mean values of each parameter were calculated and correlations made between glenoid and acromial dimensions. The shapes of the acromion were classified as curved or flat and that of scapula notch classified as either L-shaped or U-shaped.

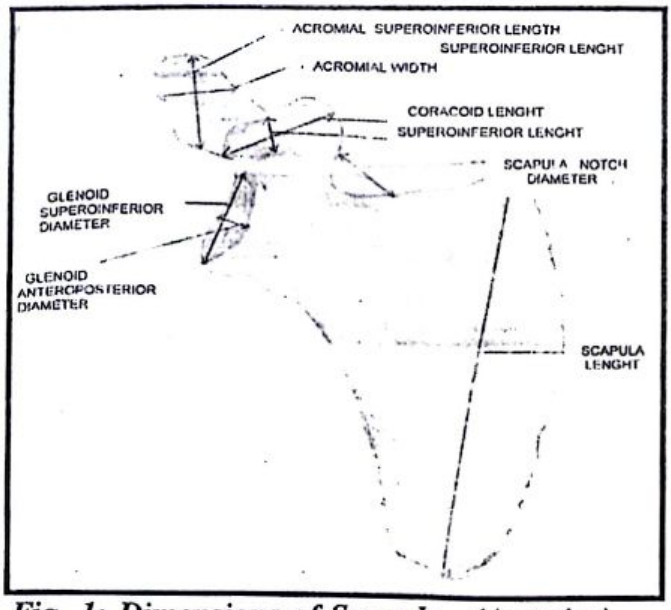

Fig. 1: Dimensions of Scapula (Anterior)

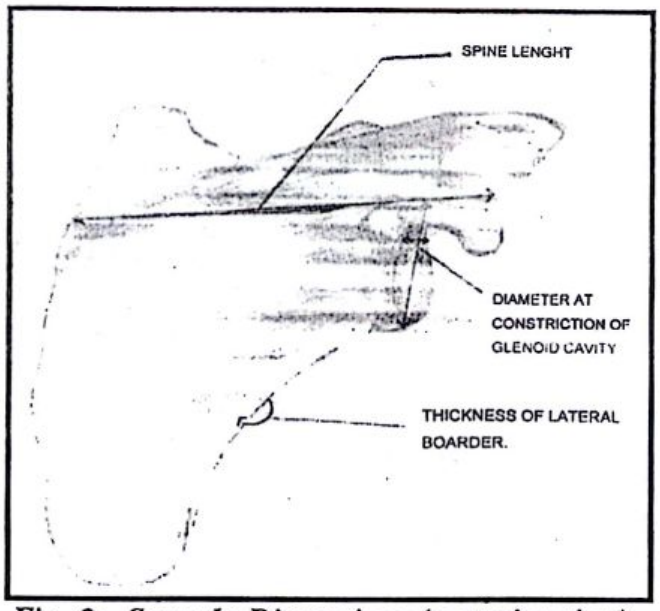

Fig. 2: Scapula Dimensions (posterior view)

RESULTS

The results are shown in the below

S/N	Parameters	Mean measurements (MM)	Range
1	Length of scapula	146.24 ± 6.78mm	131.0 – 157.0mm
2	Thickness of medial boarder	3.61 ± 0.32mm	3.00 – 4.05
3	Base of scapula notch to superior rim of glenoid cavity	29.28 ± 3.56	25.50 – 38.00
4	Spine length	126.83 ± 7.29mm	115.50 – 133.00
5	Width of spine at 1cm from the medial edge	8.38 ± 1.51mm	4.50 – 11.00
6	Width of spine at 4cm from medial edge	18.49 ± 3.07mm	14.20 – 22.50mm
7	Glenoid dimensions:		
	Anteroposterior diameter	26.54 ± 1.86mm	23.50 – 29.50mm
	Supenorinferior diameter	37.72 ± 1.65mm	33.00 – 41.00mm
	Diameter at constriction	19.58 ± 1.37mm	16.50 – 21.50mm
8	Acromial dimensions:		
	Superioinferior length	45.46 ± 4.03mm	37.50 – 54.00mm
	Acromial width	21.91 ± 2.07mm	18.50 – 27.00mm
	Thickness	7.36 ± 1.30mm	5.00 – 9.00mm
9	Coracoid dimensions:		
	Length	39.20 ± 2.67mm	35.00 – 44.50mm
	Superiorinferior thickness	9.30 ± 2.12mm	6.00 – 13.50mm
	Anteroposterior (width)	14.48 ± 1.36mm	13.50 – 16.00mm
10	Diameter of scapula notch	14.90 ± 2.94	10.00 – 21.00mm
11	Thickness of lateral boarder	11.72 ± 1.23	9.50 – 15.00mm

Other results show that the scapula notch was shaped like a "U" in 52% of scapula and "L" shaped in 48%; the acromion was curved in 92% of scapula and flat in 8%. Also Pearson's correlation evinced that Glenoid anteroposterior diameter was related to its superiorinferior diameter ($p=0.041$), Diameter at constriction of glenoid cavity ($p=0.000$), acromial superoinferior length ($p=0.01$) and acromial width ($p=0.02$) at $P<0.05$. The acromial thickness did not correlate with other acromial measurements and all glenoid dimensions.

DISCUSSION

This study was directed mainly towards investigating the normal values of scapula dimensions of Nigerians living in the south-east zone.

Measurements by Von Schroeder et al (2001) showed that for a Caucasian community, the mean values of parameters like length of scapula (155 $\pm$ 16mm); Distance from the base of scapula notch to the superior rim of glenoid (32 $\pm$ 3mm); length of spine (134 $\pm$ 12mm) and acromial dimensions (48 $\pm$ 5 x 22 $\pm$ 4mm 8.9 $\pm$ mm thick) were higher than the values gotten in this study (146.24 $\pm$ 6.78; 29.28 $\pm$ 3.56; 126.83 $\pm$ 7.29; 45.46 v 4.03 x 21.91 and 7.36 $\pm$ 1.30 thick respectively). This could be attributed to one of the racial differences between blacks and Caucasians and should be noted and applied by surgeons performing hardware fixation, drill hole placement and prosthetic positioning of scapula in our immediate environment. These scapula dimensions may serve as a peredictive factor in the pattern of scapula humeral disorders observed in our immediate environment.

Correlations observed between Glenoid dimensions [Superioinferior diameter (AP)] with acromial length and width show that they are factors in the stability of the shoulder joint and may be jointly involved in maintaining subacromial clearance. The non-relationship of acromial thickness shows that it is not a likely factor in shoulder stability and maintenance of subacromial clearance.

Results equally show that 92% of acromion are curved. This value is higher than measurements by Von Schroeder et al (2001) where 63% of scapulae had curved acromial processes. The shape of the acromion could be a factor in the subacromial space clearance during different orientations of the scapula and if there is a decrease of subacromial clearance in upward rotation (Karduna et al, 2005) there could be a possible further decrease in subacromial clearance in individuals bearing highly curved or hooked acromial processes, thus, increasing the likely occurrence of impingement syndromes.

52% of the scapula had U-shaped scapula notch and the shape of the notch could be a factor in the occurrence of a possible suprascapula entrapment neuropathy.

The findings from this study will serve as a tool for surgeons in open reduction and internal fixation of significantly displaced scapula fractures.

ACKNOWLEDGEMENT

Our acknowledgement goes to Uzoagbara, M (Chief Technologist of the Department of Human Anatomy, Faculty of Basic Medical Sciences, Ebonyi STAte University, Abakaliki) for his technical experience that made possible the extraction and processing of bones used in this study.

REFERENCES

Didia B C, Nwajagu G I, Ulonnam C C (2002). Femoral Intercondylar notch geometry of Nigerians. J. Expt. And Clin Anat. 2(1): 1-8.

Gumina S, Postatchini F, Orsina L, Cinotti G (1999). The morphometry of the Coracoid process-its aetiologic role in subcoracoid impingement syndrome Int Othop. 23(4): 198- 201.

Gumpel-Pinot M: Muscles and Skeleton of limbs and body wall. In: Ledouarin, N, Mclaren A (eds) Chimeras in developmental Biology Academic Press: London. 1984. Pp. 281-310.

Karduna A R, Kerner P J, Lazarus M D (2005). Contact forces in the subacromial space: Effects Scapular orientation. 14 (4) 393-399.

Mallon W J, Brown H R, Vogler J B, Martinez S (1992). Radiographic and geometric Anatomy of the Scapula. Clin Orthop. 277: 142-154.

Von Schroeder H P, Kuiper S, Botte M J (2001). Osseous Anatomy of the Scapula. Clin Orthop and related research. (383): 131-139.